Supplementary Information

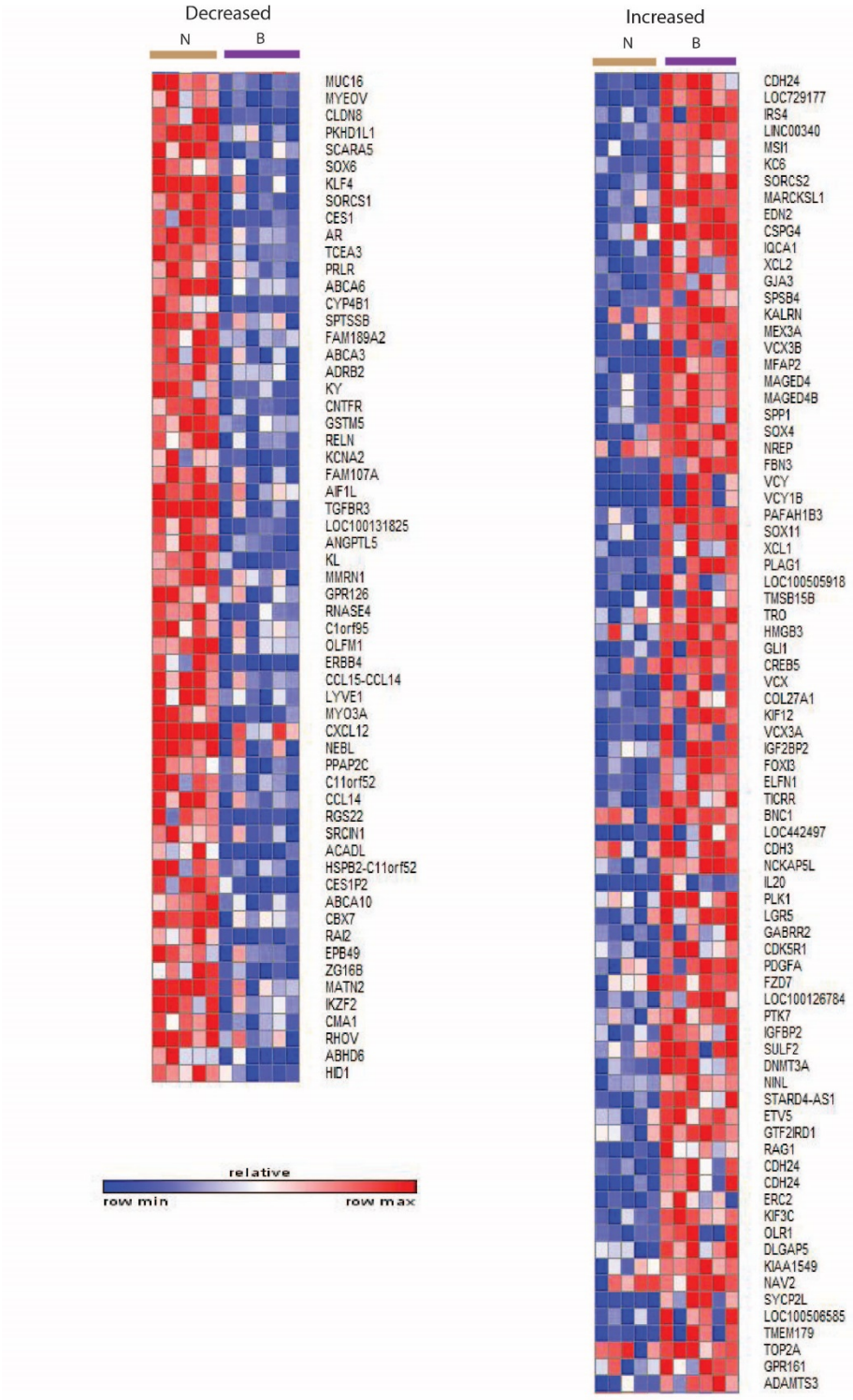

Supplemental Figure 1: Core gene signature for advanced BCCs. N represents normal skin samples and B represents advanced basal cell cancer. Blue color indicates genes with relative decreased expression and red color indicates genes with relative increased expression after mean centering. Further details are available in Table S1.

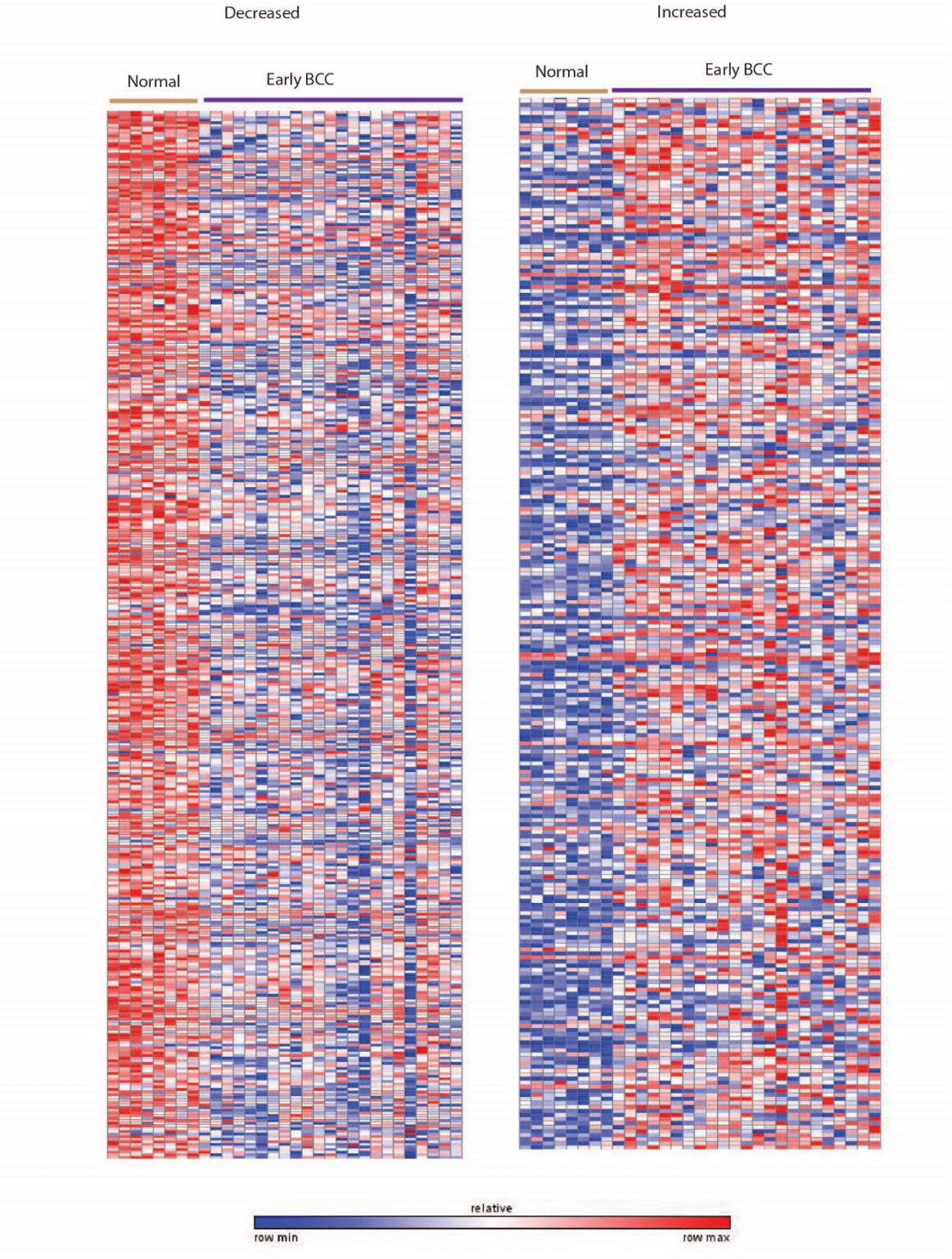

Supplemental Figure 2: Core gene signature for early BCCs. Blue color indicates genes with relative decreased expression and red with relative increased expression after mean centering. Further details and list of individual genes are available in Table S2.

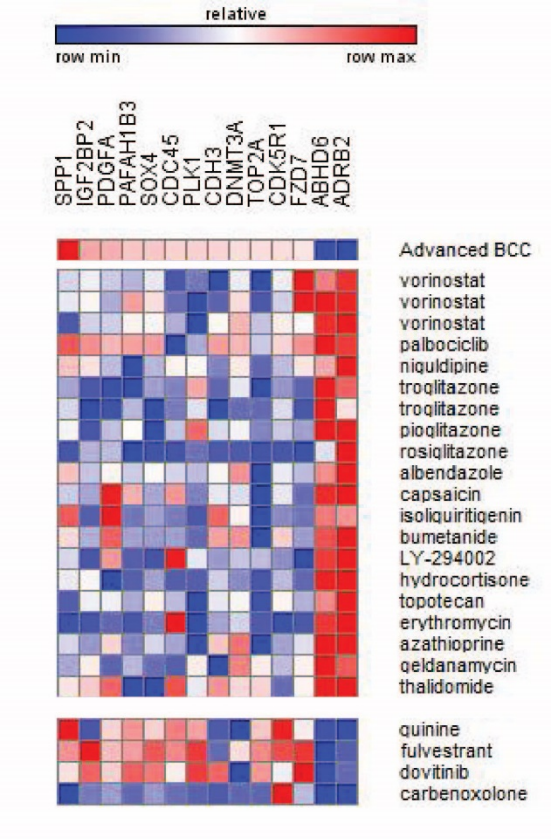

Supplemental Figure 3: LINCS landmark genes with altered expression in advanced BCC. All predicted drugs are displayed on the right. Some drugs are listed multiple times due to exposures at multiple doses. Quinine, fulvestrant, dovitinib, and carbenoxolone have concordant expression with BCC and are not predicted therapeutics (bottom panel). These are displayed for comparison purposes.

-

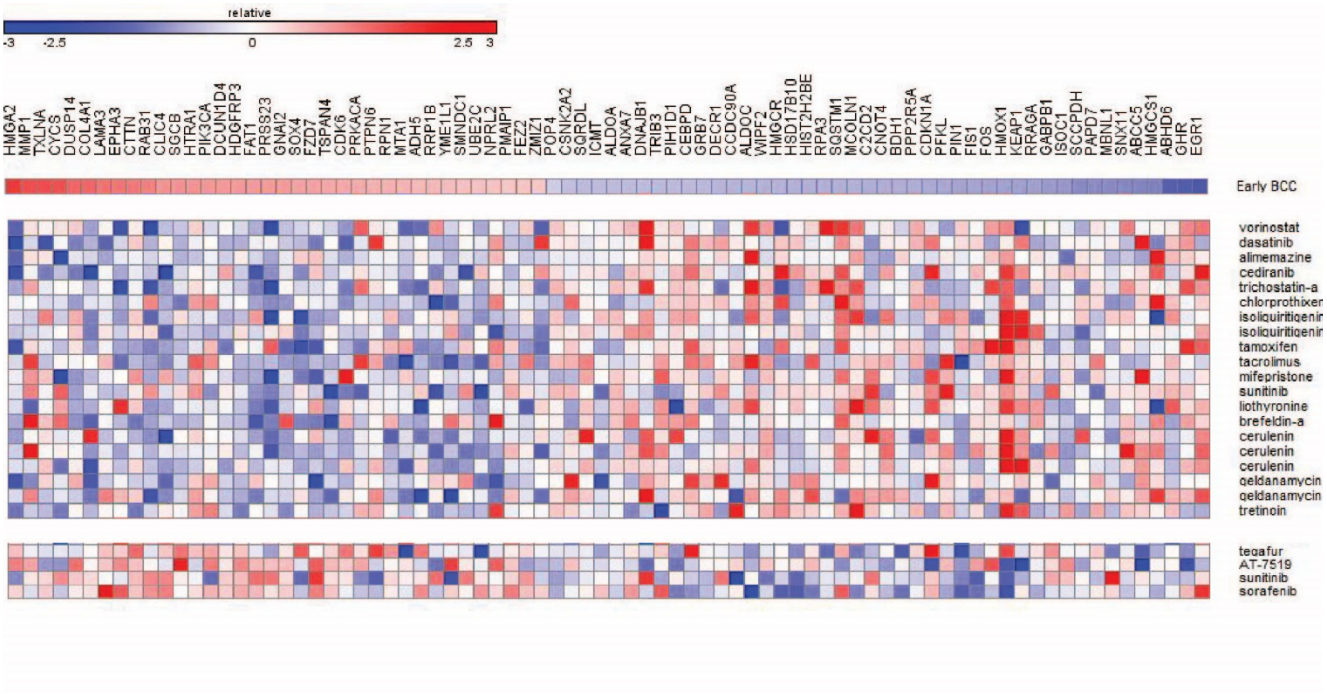

Supplemental Figure 4: LINCS landmark genes with altered expression in early BCC. All predicted drugs are displayed on the right. Some drugs are listed multiple times due to exposures at multiple doses. Tegafur, AT-7519, sunitinib and sorafenib have concordant expression with BCC and are not predicted therapeutics (bottom panel). These are displayed for comparison purposes.

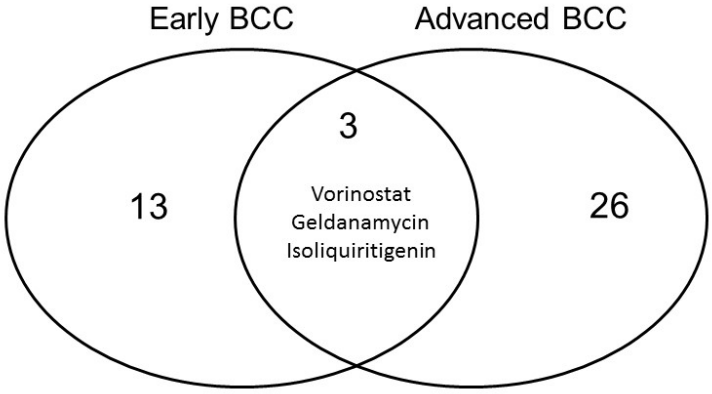

Supplemental Figure 5: Intersection of predicted therapeutics for advanced BCC and early BCC gene sets identifies three common predicted therapeutics, including vorinostat. More details can be found in Table S3-S4.

A

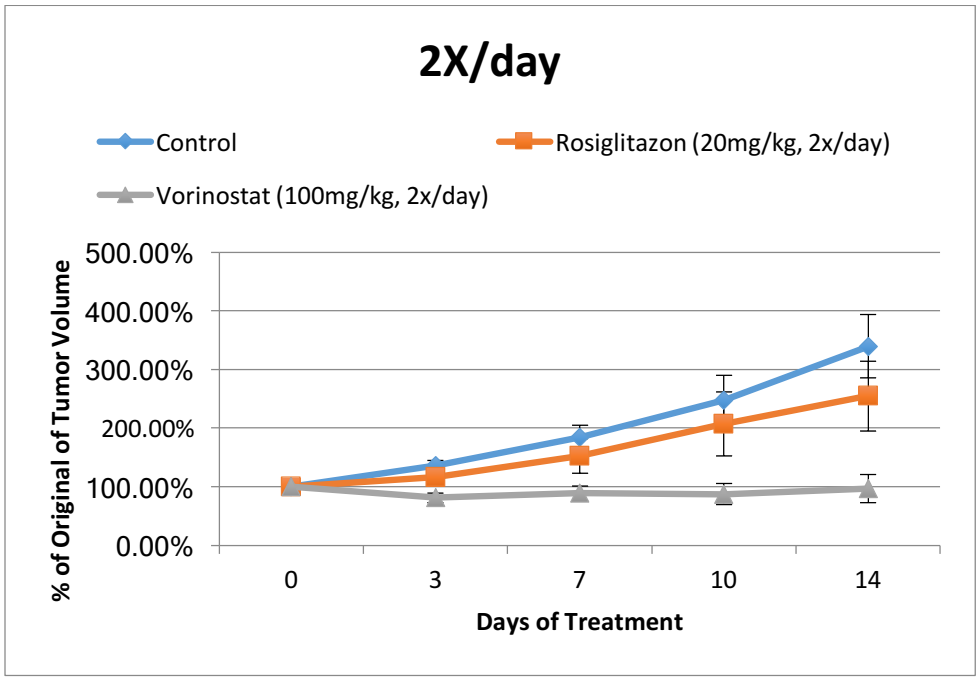

B

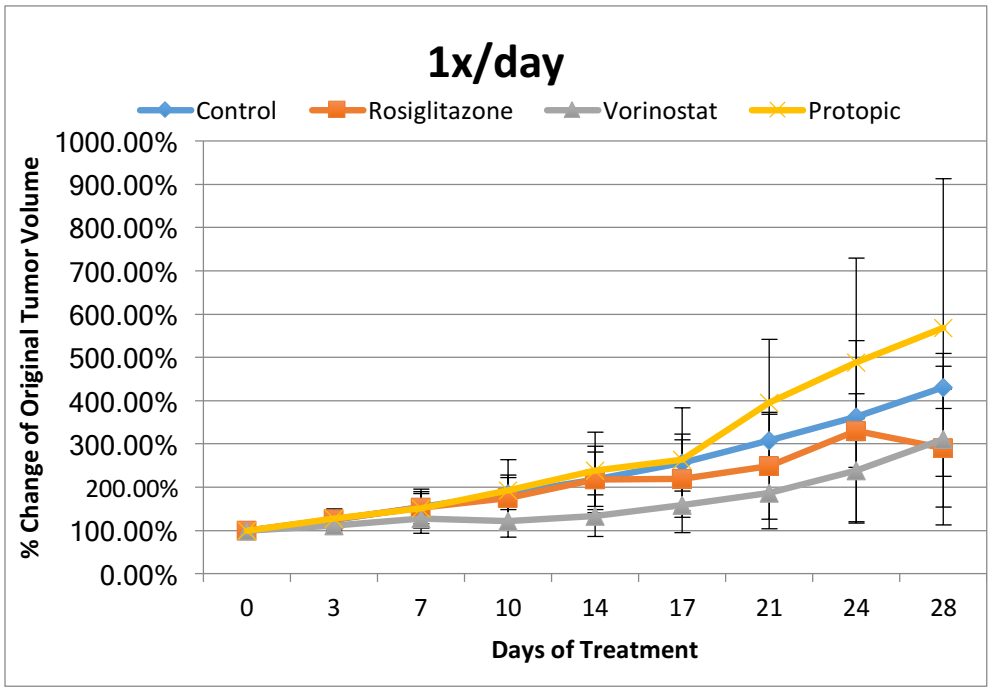

Supplemental Figure 6: Screen of top repositioning hits. Allografted mBCC treated 2X/day (**a**) or 1X/day (**b**), and tumor volume measured over time. Protopic represents topical tacrolimus. Control n=6(**a**) or 7(**b**), Rosiglitazone n=7(**a**) or 5(**b**), Vorinostat n=8(**a**) or 5(**b**), Protopic n=6. Error bars measure standard deviation.

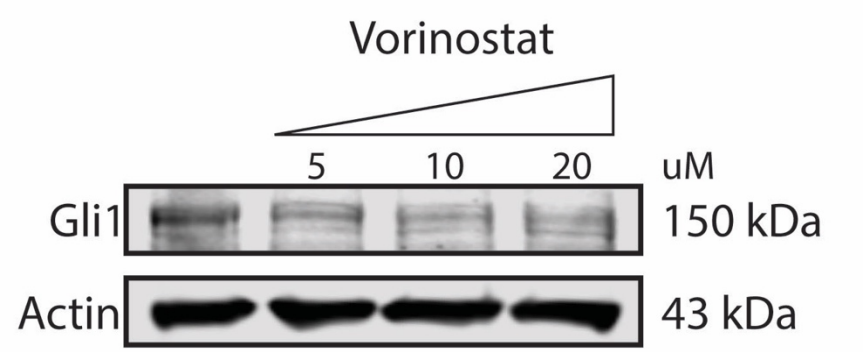

Supplemental Figure 7: Western blot of Gli1 protein following vorinostat treatment. Whole cell extract collected from ASZ cells withdrawn from serum and treated with vorinostat or vehicle for 16hrs.

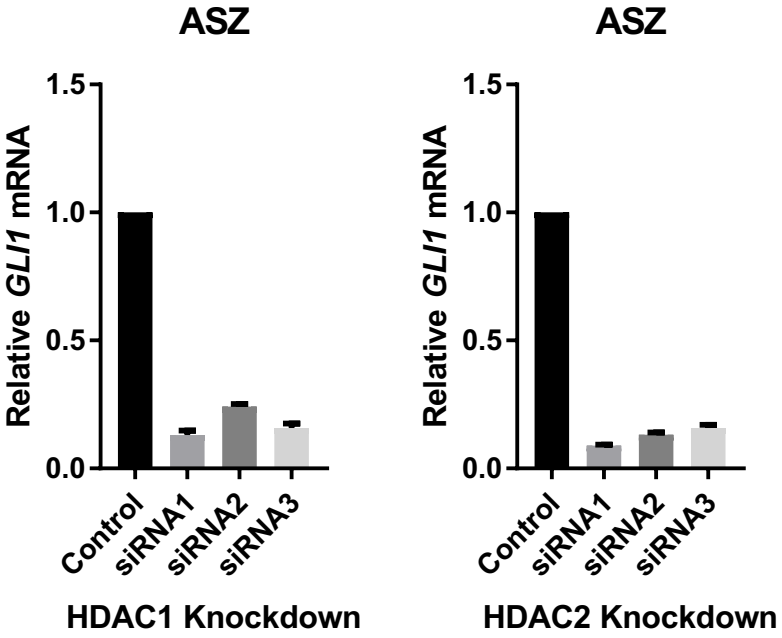

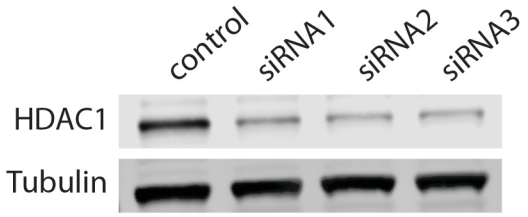

Supplementary Figure 8: Genetic depletion of HDAC1/2 mirrors vorinostat treatment. Knockdowns of HDAC1 and HDAC2 by three unique siRNAs transfected into ASZ result in hedgehog inhibition as assayed qRT-PCR of *GLI1* transcript normalized to *HPRT1* (n=9). Knockdown confirmed by western blot.

A

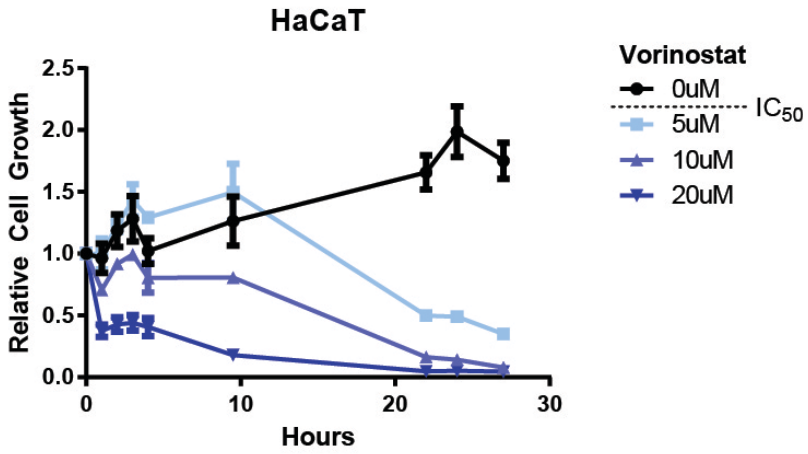

B

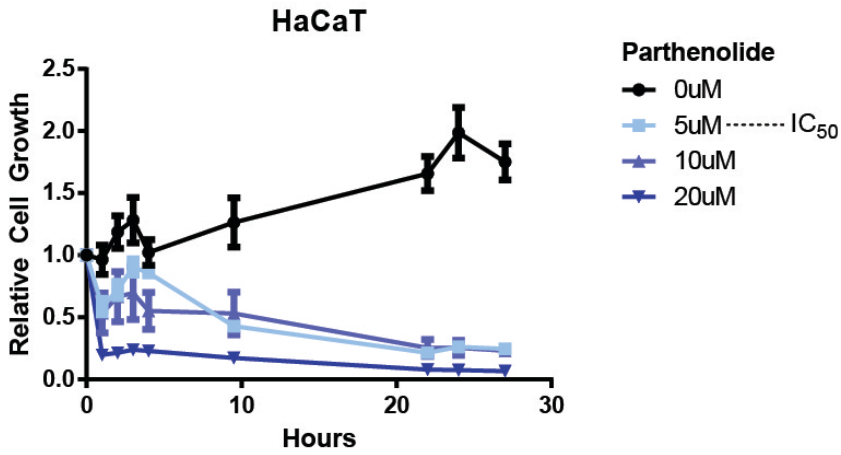

Supplemental Figure 9: High Dose HDAC inhibitors toxic to control cell line. HaCaT cells treated with indicated doses of Vorinostat (a) or Parthenolide (b) and cell growth measured by Real Time Glo reagent (n=3).

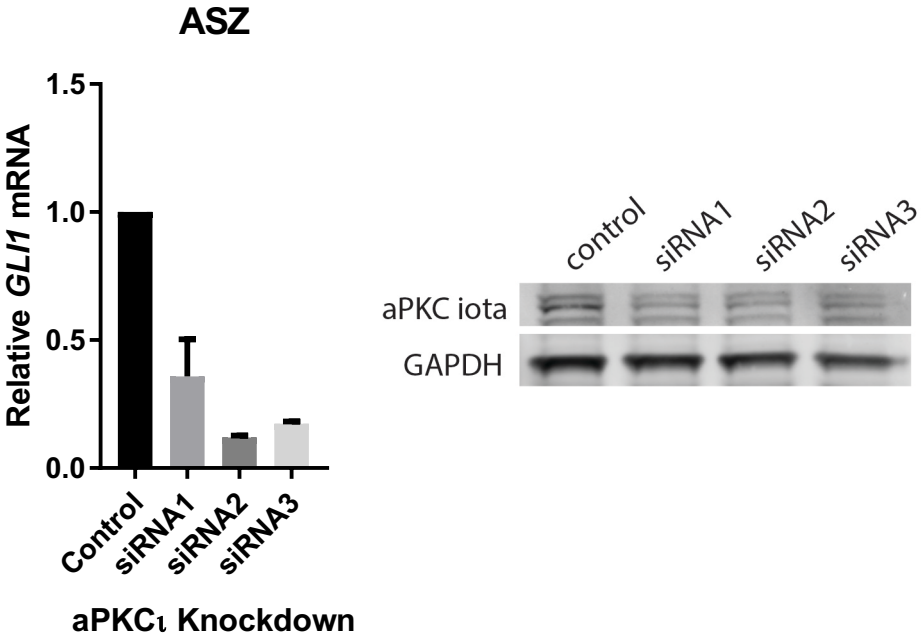

Supplementary Figure 10: Genetic depletion of $aPKC_{\iota}$ inhibits hedgehog pathway output. Knockdowns of $aPKC_{\iota}$ by three unique siRNAs transfected into ASZ result in hedgehog inhibition as assayed qRT-PCR of *GLI1* transcript normalized to *HPRT1* (n=9). Knockdown confirmed by western blot.

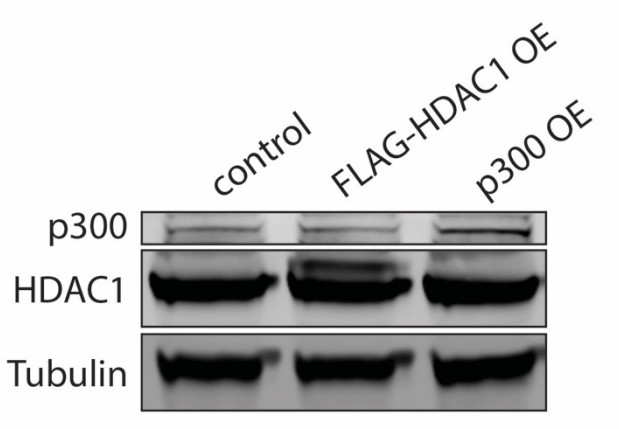

Supplemental Figure 11: Overexpression of HDAC1 and p300. Western blot of mock transfection, FLAG-HDAC1, or p300 overexpression. Exogenous HDAC1 demonstrates supershifting over endogenous protein due to FLAG epitope.

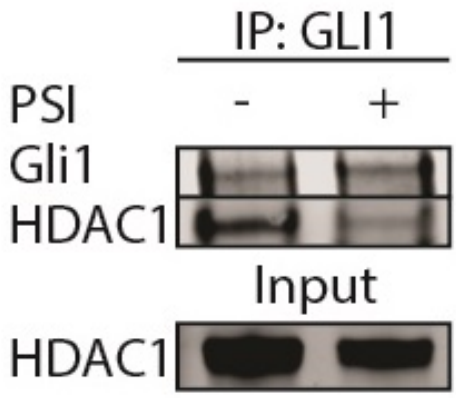

Supplemental Figure 12: Endogenous Gli1 IP in ASZ. The Gli1-HDAC1 interaction is lost following aPKC inhibition.

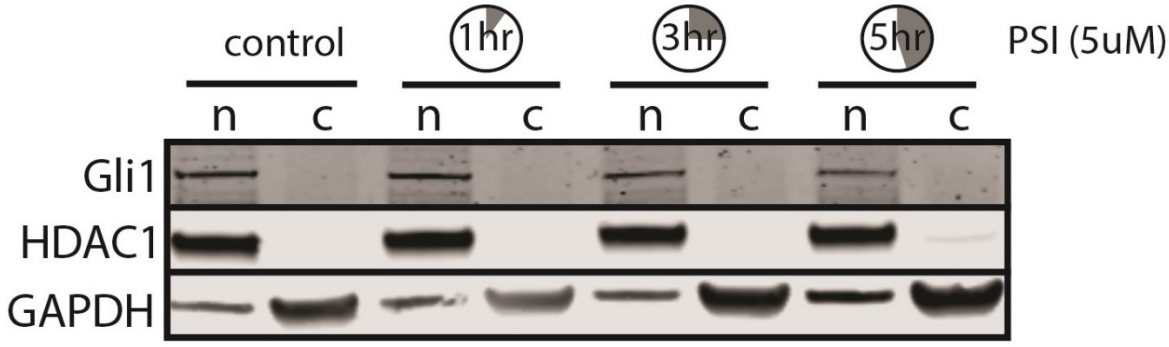

Supplemental Figure 13: PSI does not disturb GLI1's nuclear localization. Nuclear-cytoplasmic fractionation of ASZ following PSI treatment.

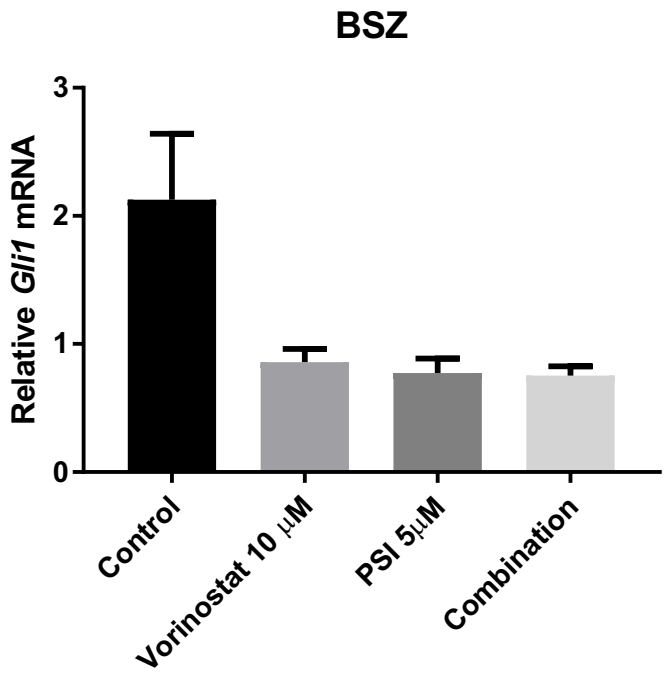

Supplemental Figure 14: BSZ cells subject to HDAC and aPKC inhibition. Cells were withdrawn from serum and drug treated overnight (16hr). qRT-PCR of *Gli1* normalized against *HPRT1* demonstrates robust response to both inhibitors. Data reflects three biological and three technical replicates each (n=9).

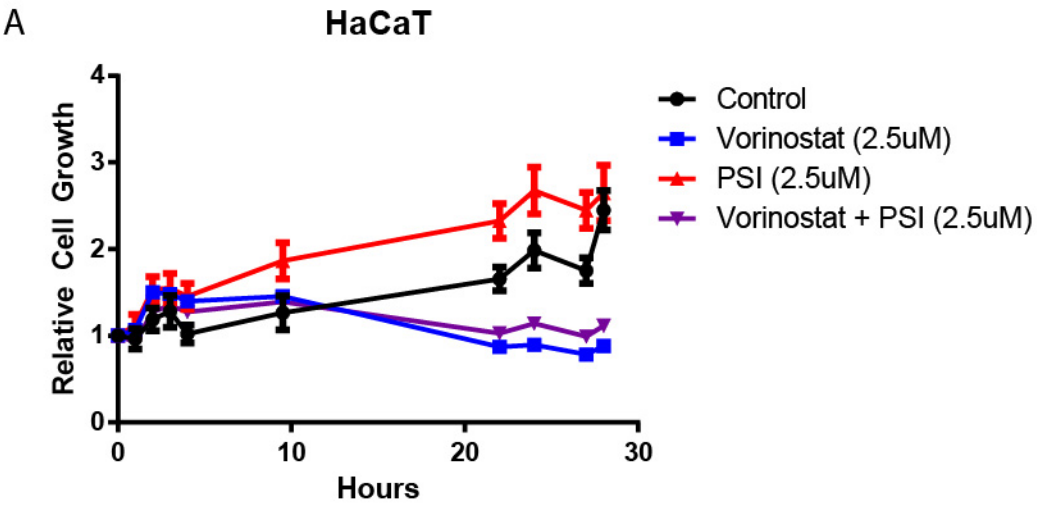

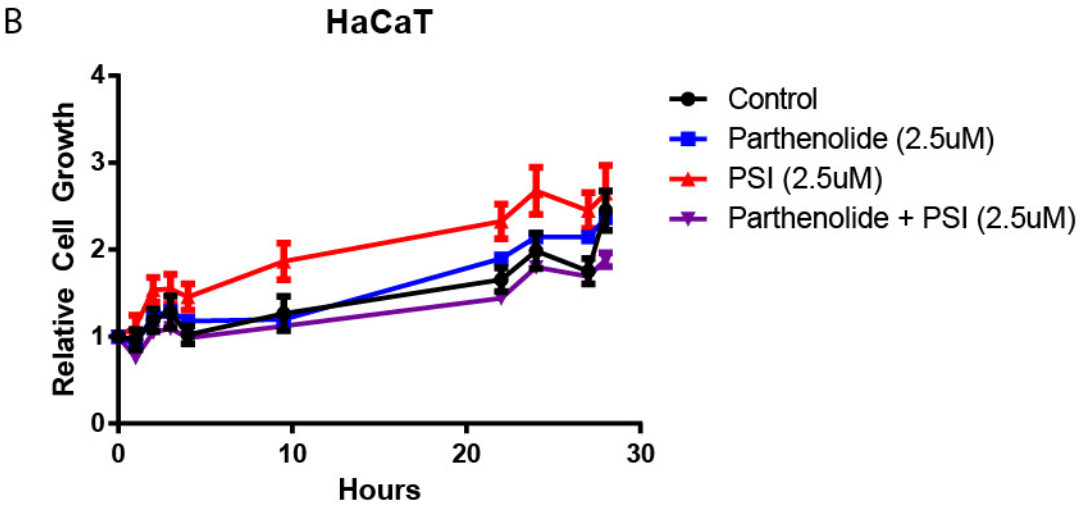

Supplemental Figure 15: Low dose combination therapy does not kill control cells. HaCaT cells treated with low dose combination therapy displayed normal growth as measured by Real Time Glo reagent (n=3).

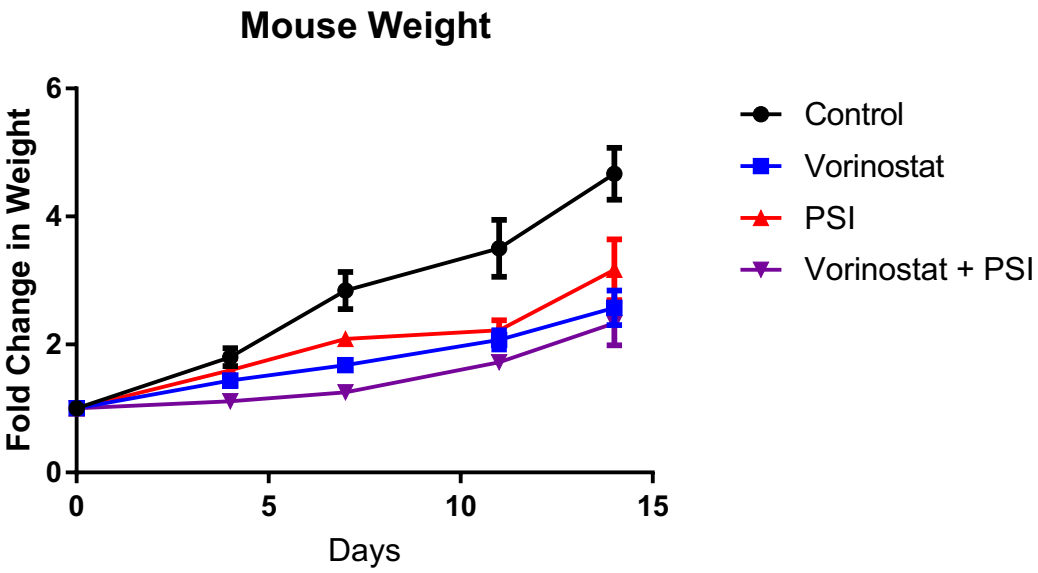

Supplemental Figure 16: Mice weight changes following drug therapy. Combination therapy yielded no additional weight loss in comparison to monotherapy (n=4).

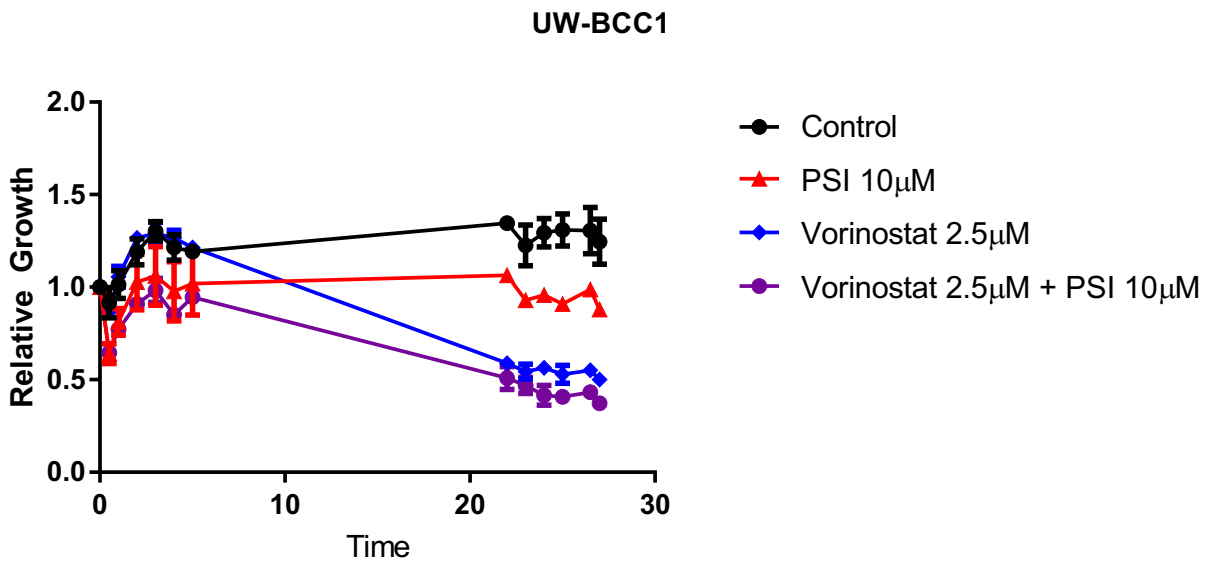

Supplemental Figure 17: UW-BCC1 viability measured during drug treatment. BSC1 cells withdrawn from serum were subject to drug treatment. Viability measured by Real Time Glo reagent. N=3, error bars represent standard error.

TAT-PSI: GRKKRRQRRRCDMAEHSIYRRGARRWRKL

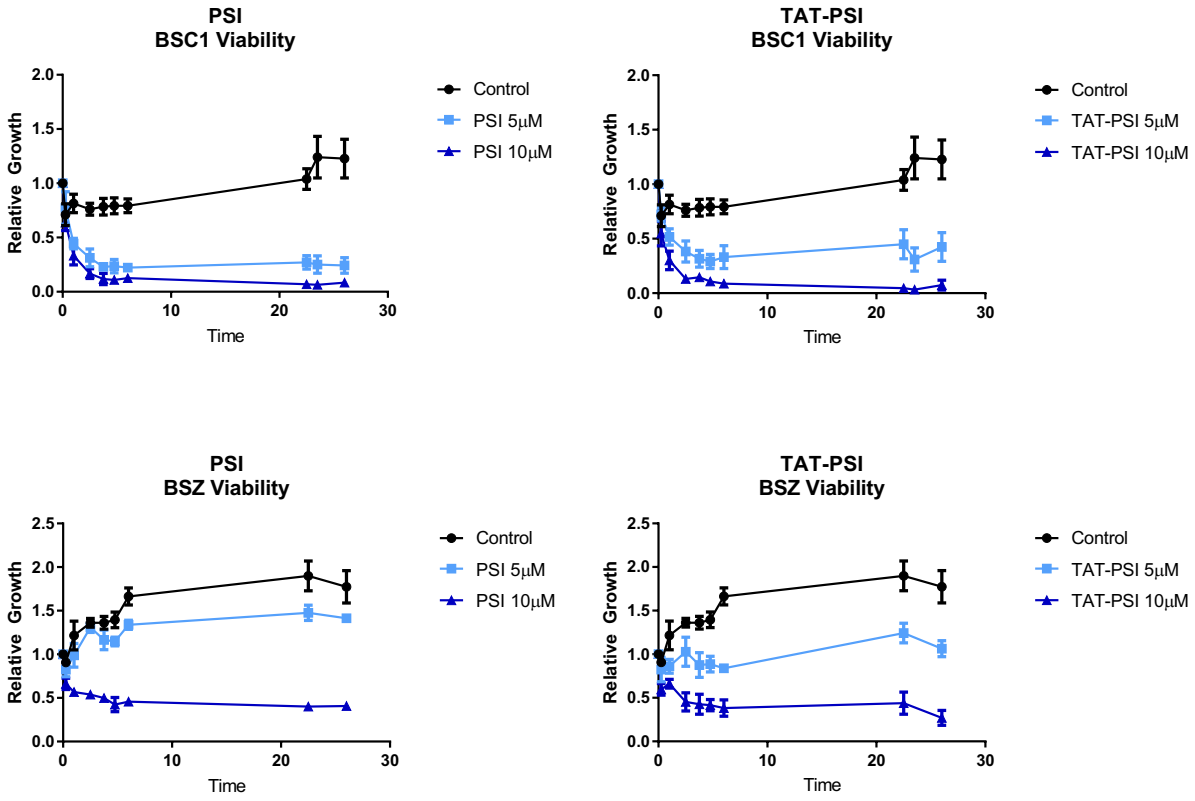

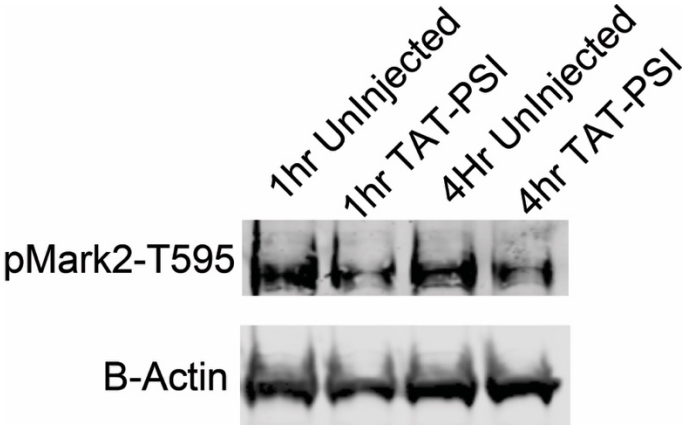

Supplemental Figure 18: TAT-PSI validation. Top: peptide sequence of TAT-PSI illustrated with TAT peptide colored green and PSI peptide colored red. Middle: viability measured by Real Time Glo of two BCC cell lines (BSZ and BSC1) to TAT-PSI or PSI of equivalent doses demonstrates they act similarly. Bottom: western blot of aPKC$_{\iota}$ target Mark2 phosphorylation T595 (pMARK2) and loading control actin following TAT-PSI administration in mice tissue.

Replicate 1

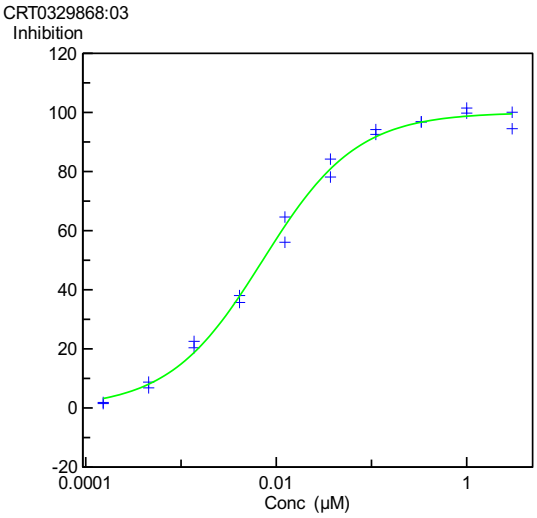

Replicate 2

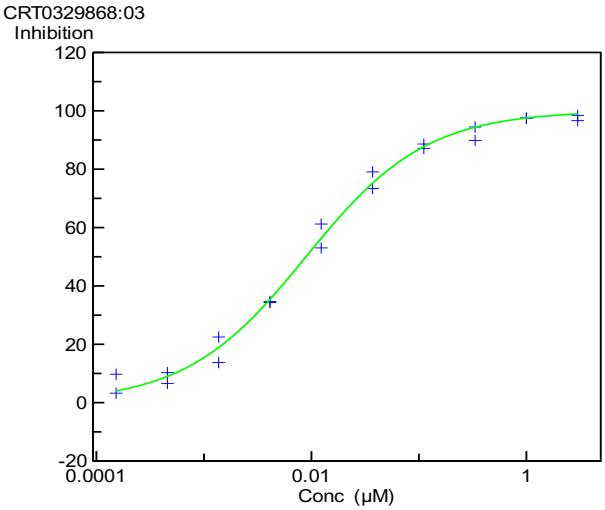

Replicate 3

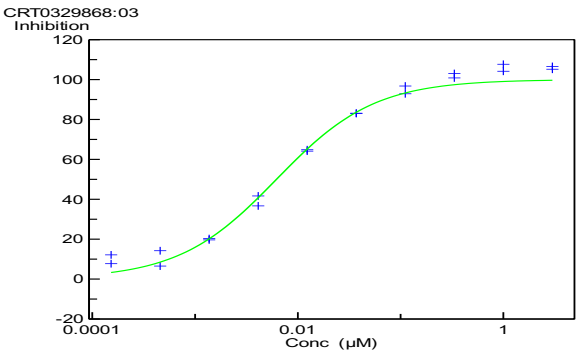

Replicate 4

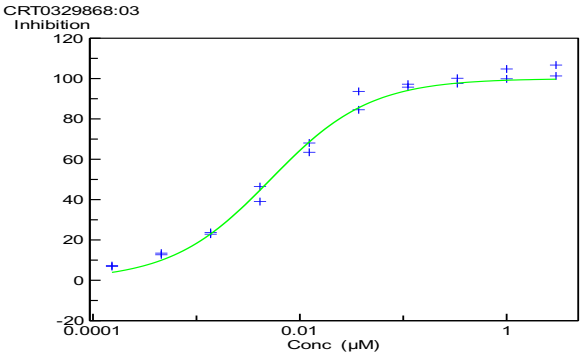

Replicates	IC_{50} (nM)
1	8.141462802
2	8.050122296
3	8.207608311
4	8.283162277

Supplemental Figure 19: Biochemical IC50 of CRT0329868. Four replicates of *in vitro* kinase assay of recombinant human baculovirus-expressed full-length PKCι was measured using the IMAP® fluorescence polarization (FP) progressive binding system. IC50 values were calculated by plotting percent inhibition versus log10 of the concentration of compound and fitting to the 4-parameter logistic model.

Replicate 1 (IC_{50}: 16nM)

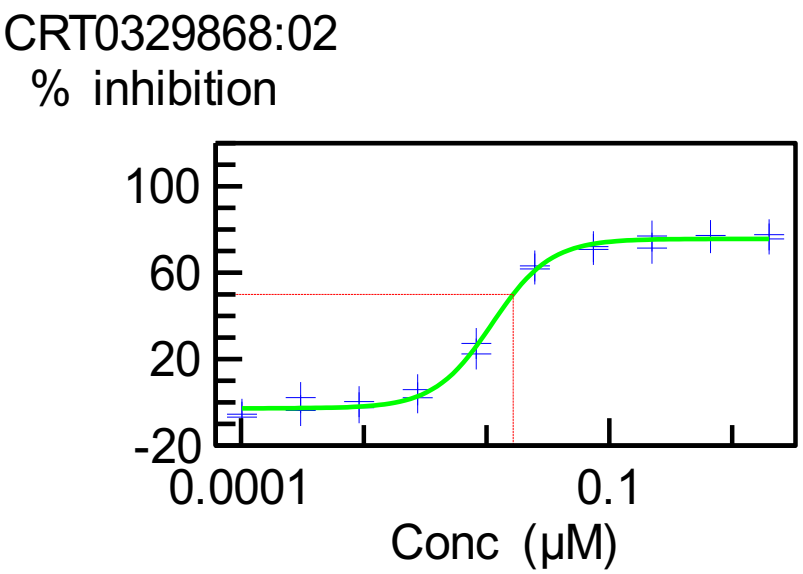

Replicate 2 (IC_{50}: 32nM)

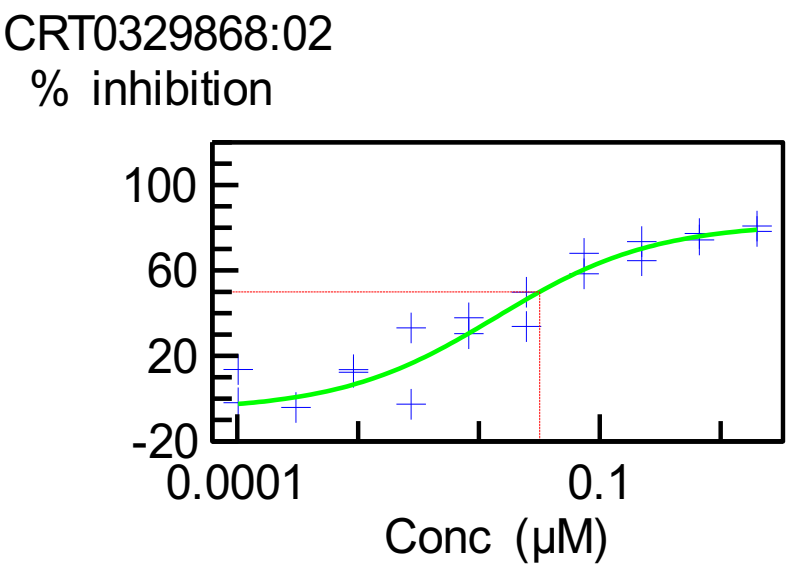

Supplementary Figure 20: Cellular IC_{50} of CRT0329868. Representative inhibition curves of aPKCι inhibition by CRT0329868 in H460 cells assayed by ELISA based detection of LLGL2 phosphorylation.

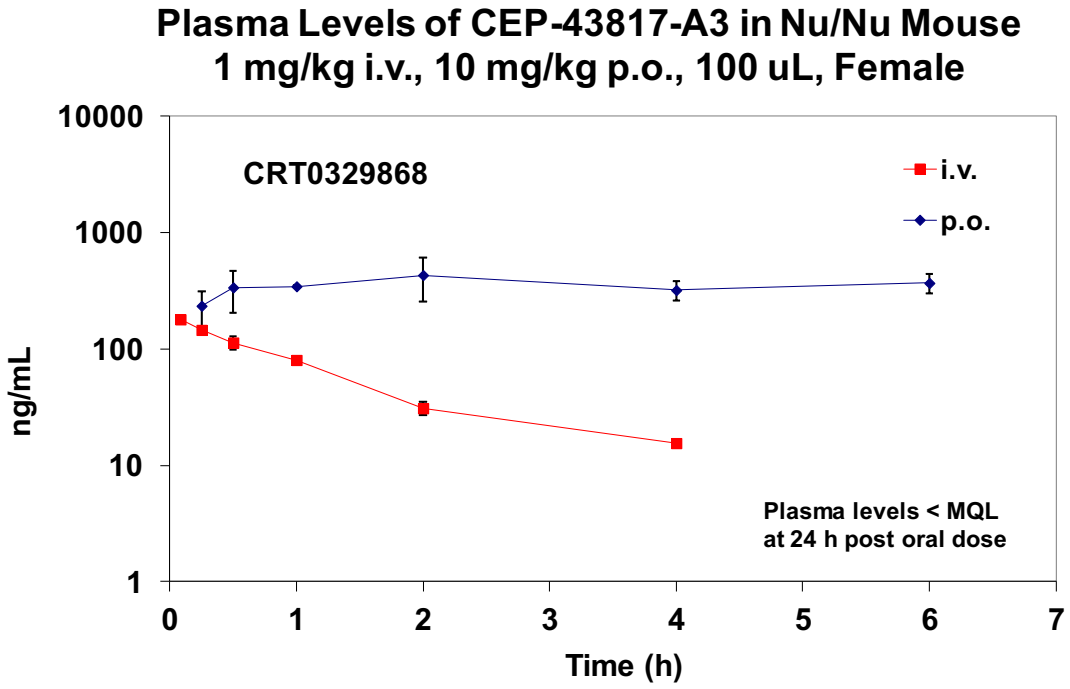

CEP-43817-A3	1 mg/kg i.v.	CRT0329868	10 mg/kg p.o.
$t_{1/2}$, h	1.1	$C_{max,}$ ng/mL	433
AUC_{0-t}, ng*h/mL	227	$T_{max,}$ h	2
$AUC_{0-\infty}$, ng*h/mL	253	AUC_{0-6}, ng*h/mL	2110
V, L/kg	6.5	$AUC_{0-\infty}$, ng*h/mL	2517
CL, mL/min/kg	67	$t_{1/2}$, h	>3
Nu/Nu Female, Mean, n=3 / time point		6 h Bioavailability, %	99

Supplementary Figure 21: Pharmacokinetics of CRT0329868 (CEP-43817-A3). CRT032986 administered by I.V. and oral as indicated. Plasma levels measured over 6hrs.

Table S1-6: Excel File Included (Table >1 page)

Table S1: Differential gene expression in advanced BCCs as compared to normal skin

Table S2: Differential gene expression in early BCCs as compared to normal skin

Table S3: Drug Repositioning for predicted therapeutics for advanced BCC

Table S4: Drug Repositioning for predicted therapeutics for early BCC

Table S5: Differential gene expression in PSI treated BCC cells as compared to control

Table S6: LINCS analysis showing expression correlation of chemical perturbagens with PSI

Table S7: RBC and Plates of Mice Treated with HDAC and aPKC inhibitors.

ID:	RBC	Plates
Reference Range	7.0 - 8.8	675 - 1338
CONTROL 619	9.03	1966
CONTROL 623	6.24	824
VORI 622	8.31	362
VORI 626	3.94	22
PSI 627	6.46	1742
PSI 625	7.78	55
COMBO 624	7.91	537
COMBS 618	9.01	1218